THE JOURNAL OF BIOLOGICAL CHEMISTRY VOL. 285, NO. 44, pp. 33788–33796, October 29, 2010

Active Site Metal Ion in UDP-3-*O*-((*R*)-3-Hydroxymyristoyl)-*N*-acetylglucosamine Deacetylase (LpxC) Switches between Fe(II) and Zn(II) Depending on Cellular Conditions*[S]

Received for publication, May 21, 2010, and in revised form, August 5, 2010 Published, JBC Papers in Press, August 13, 2010, DOI 10.1074/jbc.M110.147173

Samuel G. Gattis[‡], Marcy Hernick[§1], and Carol A. Fierke[‡§2]

From the Departments of [‡]Biological Chemistry and [§]Chemistry, University of Michigan, Ann Arbor, Michigan 48109

UDP-3-*O*-((*R*)-3-hydroxymyristoyl)-*N*-acetylglucosamine deacetylase (LpxC) catalyzes the deacetylation of UDP-3-*O*-((*R*)-3-hydroxymyristoyl)-*N*-acetylglucosamine to form UDP-3-*O*-myristoylglucosamine and acetate in Gram-negative bacteria. This second, and committed, step in lipid A biosynthesis is a target for antibiotic development. LpxC was previously identified as a mononuclear Zn(II) metalloenzyme; however, LpxC is 6–8-fold more active with the oxygen-sensitive Fe(II) cofactor (Hernick, M., Gattis, S. G., Penner-Hahn, J. E., and Fierke, C. A. (2010) *Biochemistry* 49, 2246–2255). To analyze the native metal cofactor bound to LpxC, we developed a pulldown method to rapidly purify tagged LpxC under anaerobic conditions. The metal bound to LpxC purified from *Escherichia coli* grown in minimal medium is mainly Fe(II). However, the ratio of iron/zinc bound to LpxC varies with the metal content of the medium. Furthermore, the iron/zinc ratio bound to native LpxC, determined by activity assays, has a similar dependence on the growth conditions. LpxC has significantly higher affinity for Zn(II) compared with Fe(II) with K_D values of 60 ± 20 pM and 110 ± 40 nM, respectively. However, *in vivo* concentrations of readily exchangeable iron are significantly higher than zinc, suggesting that Fe(II) is the thermodynamically favored metal cofactor for LpxC under cellular conditions. These data indicate that LpxC expressed in *E. coli* grown in standard medium predominantly exists as the Fe(II)-enzyme. However, the metal cofactor in LpxC can switch between iron and zinc in response to perturbations in available metal ions. This alteration may be important for regulating the LpxC activity upon changes in environmental conditions and may be a general mechanism of regulating the activity of metalloenzymes.

Gram-negative bacteria are important targets in the continuing fight against antibiotic-resistant infections. The development of new antibiotics to treat infections caused by resistant organisms is critically needed and will require novel targets. One potential source of targets in Gram-negative bacteria is the lipid A biosynthetic pathway (Fig. 1*A*) (1, 2), an essential building block of lipopolysaccharides (LPS) that make up the outer leaflet surrounding the cell wall in Gram-negative bacteria (2–4). In addition to being essential for cell viability, LPS are also referred to as endotoxins (2, 4, 5) and are responsible for immunogenic stimulation in septic shock that can lead to a number of deleterious effects, including severe hypotension, multiple organ dysfunction, and death (5). Consequently, inhibitors of lipid A biosynthesis have the potential to serve as both antibiotics and antiendotoxins (6). The UDP-3-*O*-((*R*)-3-hydroxymyristoyl)-*N*-acetylglucosamine deacetylase (LpxC)[3] catalyzes the committed and second overall step in lipid A biosynthesis, the hydrolysis of UDP-3-*O*-myristoyl-*N*-acetylglucosamine to UDP-3-*O*-myristoyl-glucosamine and acetate (Fig. 1) (7–10). Consequently, inhibitors of LpxC are an active area of drug development (11–14).

LpxC was previously identified as a mononuclear Zn(II) metalloenzyme (Fig. 1*B*) (15) that also contains a weaker, inhibitory metal ion-binding site. This catalytic metal ion binds and polarizes an inner sphere water molecule that is activated by general base catalysis to serve as the nucleophile for hydrolysis of the acetyl substrate (Fig. 1*C*) (16, 17). However, recent evidence has shown that LpxC is more active with Fe(II) as its metal ion cofactor compared with Zn(II) (18). This increase in activity may correlate with a change in the ground state metal geometry from 4-coordinate in ZnLpxC to 5-coordinate in the Fe(II)-enzyme (18) that facilitates catalysis by enhancing coordination and polarization of the carbonyl group of the substrate (Fig. 1*C*). Several enzymes described previously as Zn(II)-dependent enzymes have recently been reclassified as Fe(II) enzymes, including peptide deformylase, *S*-ribosylhomocysteinase, and possibly histone deacetylase 8 (HDAC8) (19–24). Iron is a highly abundant transition metal ion in cells (25, 26); however, the Fe(II) redox state that activates LpxC oxidizes to Fe(III) in air (18). Therefore, it is not yet clear which metal ion activates LpxC *in vivo*.

Both iron and zinc exist in high amounts in the cell, with total concentrations around 0.2 mM in *Escherichia coli* (26). However, the concentrations of the readily exchangeable, or "free," metal ions are vastly different. Although estimates vary, the best

* This work was supported, in whole or in part, by National Institutes of Health Grant GM40602 (to C. A. F.) and PSTP Training Grant GM07767 (to S. G. G.) from NIGMS. This work was also supported by the Cystic Fibrosis Foundation Grant HERNIC05F0 (to M. H.).

[S] The on-line version of this article (available at http://www.jbc.org) contains supplemental Figs. S1 and S2 and additional refs.

[1] Present address: Dept. of Biochemistry, Virginia Tech, Engel Hall, Blacksburg, VA 24061.

[2] To whom correspondence should be addressed. Tel.: 734-936-2678; Fax: 734-647-4865; E-mail: fierke@umich.edu.

[3] The abbreviations used are: LpxC, UDP-3-*O*-((*R*)-3-hydroxymyristoyl)-*N*-acetylglucosamine deacetylase; TCEP, triscarboxyethylphosphine; ICP-MS, inductively coupled plasma mass spectrometry; LpxC-ZZ, EcLpxC-C63A-Tev-ZZ; NTA, nitrilotriacetic acid; BisTris, 2-[bis(2-hydroxyethyl)amino]-2-(hydroxymethyl)propane-1,3-diol; Bistris propane, 1,3-bis[tris(hydroxymethyl)methylamino]propane; CDM, Chemically Defined Medium.

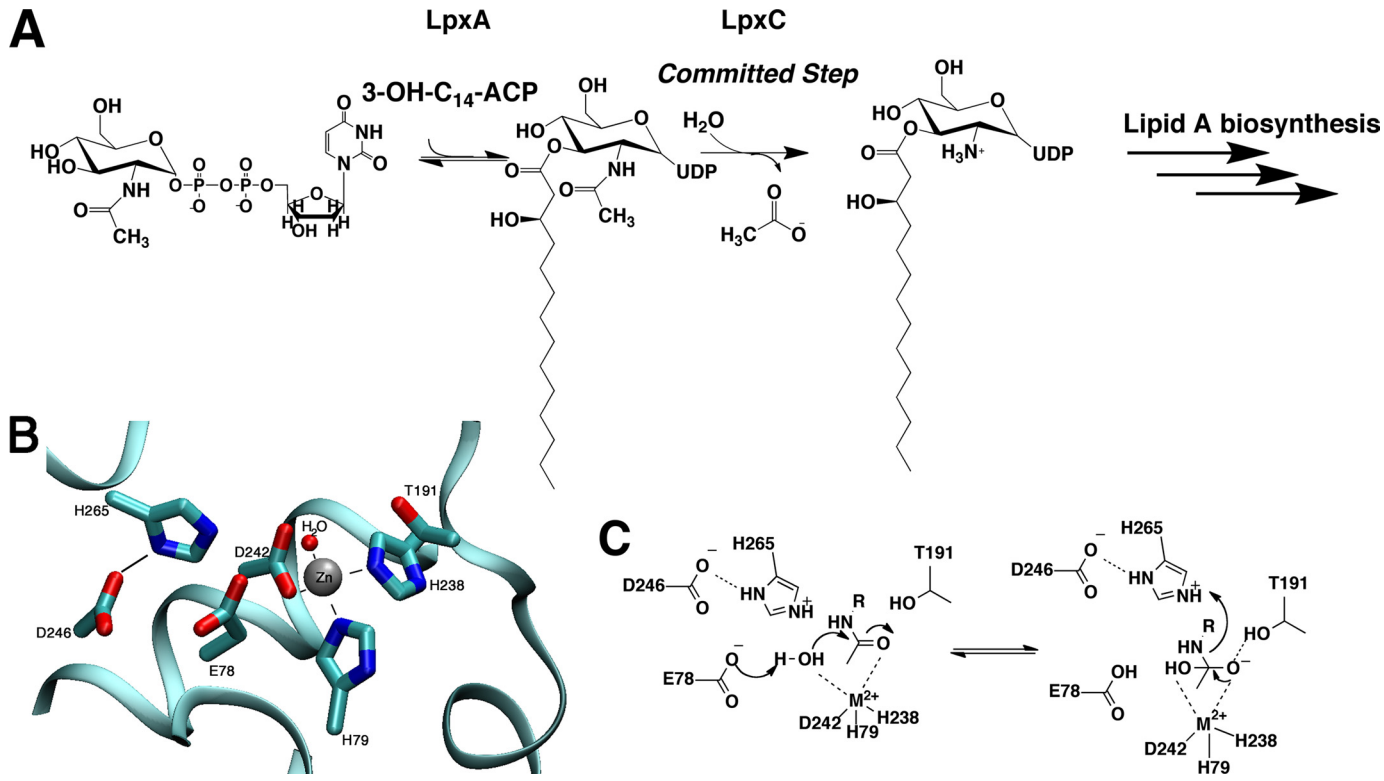

FIGURE 1. *A,* role of LpxC in lipid A biosynthesis. *B,* active site of ZnLpxC derived from Protein Data Bank code 1P42 (49). *C,* proposed chemical mechanism of LpxC catalysis (16).

data available for readily exchangeable Fe(II) and Zn(II) come from mammalian cells, where estimates indicate that $[Zn(II)_{free}]$ is picomolar (10–400 pM) (27, 28), and $[Fe(II)_{free}]$ is micromolar (0.2–6 μM) (29–32). The combination of the higher concentration of readily exchangeable Fe(II) and the enhanced reactivity of Fe(II)-bound LpxC (18) suggest that the native cofactor bound to LpxC in *E. coli* might be Fe(II) rather than Zn(II). To test this hypothesis, we developed rapid purification methods and activity assays to analyze the metal ion status of LpxC *in vivo*. Using these methods, we demonstrate that under normal growth conditions iron-bound LpxC predominates. However, the ratio of iron/zinc bound to LpxC depends on the cellular metal content. Although LpxC binds Zn(II) with much higher affinity than Fe(II), the higher cellular concentration of $Fe(II)_{free}$ contributes to the formation of Fe(II)-bound LpxC *in vivo*. In summary, these data indicate that Fe(II) is the biologically relevant cofactor for LpxC under common growth conditions, although metal switching occurs in response to metal availability. Furthermore, metal switching may be important for regulating the LpxC activity upon changes in cellular conditions.

MATERIALS AND METHODS

General Procedures, Protein Expression, and Plasmid Construction—All solutions were prepared in "metal-free" plasticware, with reagents that did not contain extraneous metal ions and/or were treated with Chelex (Bio-Rad). The metal content of solutions, reagents, and proteins was measured by inductively coupled plasma emission mass spectrometry (ICP-MS; Dr. Ted Huston, University of Michigan). LpxC and LpxC fusion proteins were overexpressed in BL21(DE3) *E. coli* transformed with pET-derived expression plasmids and purified according to published procedures using DEAE-Sepharose and Reactive Red-120 affinity dye columns (8, 15, 16). The apo-forms and single metal-bound forms of LpxC were prepared by treatment with metal chelators followed by reconstitution with Zn(II) or Fe(II) as described previously (15, 16, 18).

The pEcC63ALpxC expression plasmid encoding *E. coli* LpxC with the C63A mutation (18) was modified to encode a fusion protein between LpxC and an IgG-binding protein, termed a ZZ tag (33–35), with a tobacco etch virus protease site in the linker region between the two proteins. An NcoI restriction site was introduced at the C-terminal stop codon of LpxC by using the QuikChange mutagenesis kit (Stratagene) with the primer 5′-CCT TCA GCT GTA CTG GCA CCA TGG GGA TCC GAA TTC GAG CTC CG-3′ and its reverse complement. The ZZ tag insert was amplified using PCR from the ZZ region of the commercial vector pEZZ (Amersham Biosciences) with the introduction of XhoI and EcoRI restriction sites as well as a stop codon at the 3′ end (forward primer 1, 5′-CGA TGA ACT CGA GGA CAA CAA ATT CAA CAA AG-3′, and reverse primer 1, 5′-TAA AGA ATT CTC AGG TTT CTA GAT TCG CGT CTA CTT TCG G-3′). The DNA fragment was extended using PCR amplification to add a TEV-protease cleavage site and an NcoI restriction site using the forward primer 2, 5′-ATG ACT TGC AAC CCA TGG GAG AAC CTG TAC TTC CAG GGT CTC GAG GAC AAC-3′, and the reverse primer 1 (see above). The PCR product and pLpxC plasmid containing the

new NcoI restriction site were digested with NcoI and EcoRI and ligated together, catalyzed by T4 DNA ligase (New England Biolabs), to create the expression plasmid pEcC63ALpxC-ZZ. The plasmid sequence was verified by the University of Michigan DNA Sequencing Core. The presence of the ZZ tag does not alter the LpxC activity or product affinity. However, the activity of the LpxC-ZZ fusion protein is more sensitive to freeze/thaw cycles than the untagged LpxC (data not shown).

IgG Pulldown Experiments—*E. coli* BL21(DE3) cells transformed with pC63ALpxC-ZZ were grown in Chemically Defined Medium (CDM) (36). Protein expression was induced when the cells reached an A_{620} of 0.6 by the addition of 1 mM isopropyl β-D-thiogalactopyranoside along with the addition of either no added metals, 5–20 μM $ZnSO_4$, 5–20 μM ferric ammonium citrate, or both metal supplements, and the cells were incubated overnight at 30 °C. The cells were pelleted by centrifugation, washed once with 5 mM $CaCl_2$ and twice with 10 mM Mops, pH 7. Control experiments demonstrate that 10 mM Ca(II) has no effect on the activity of ZnLpxC or apo-LpxC. The washed cell pellets from 100 ml of growth medium were transferred to an anaerobic glove box, resuspended in 3 ml of pulldown buffer (40 mM Mops, pH 8, 150 mM NaCl, 10 mM TCEP, 0.1% Nonidet P-40), and lysed by incubation with lysozyme (1 mg/ml) at room temperature for 15–30 min. The tubes were sealed with parafilm and removed from the glove box, and the cell lysate was cleared by centrifugation (12,000 rpm, 15–30 min). The sealed tubes were transferred back into the glove box; a portion of cleared lysate (200 μl) was set aside for ICP-MS analysis, and the remaining cleared lysate was incubated with 100 μl of IgG-Sepharose beads (Sigma) for 30 min. The IgG-Sepharose beads were washed with 3× 1 ml of pulldown buffer, resuspended in 297 μl of pulldown buffer, and EcC63A LpxC and metal ions were eluted from the IgG beads by either incubation with 3 μl of AcTEV™ protease (10 units/μl, Invitrogen) or 10 mM nitric acid at room temperature overnight. The metals in the eluate were analyzed by ICP-MS. The concentration of EcC63A LpxC in the eluate was determined using the Bradford assay (Sigma) with purified LpxC as the standard. For control experiments, purified apo-LpxC-ZZ (100 μM) was reconstituted with 1 eq of either $ZnSO_4$ or $FeCl_2$ in the anaerobic glove box. The holo-LpxC (9 μM final) was then diluted into cell lysate prepared from BL21(DE3) cells transformed with the pEcC63A plasmid, encoding LpxC without a ZZ tag, and incubated for 30 min at room temperature. The lysate was then applied to IgG-agarose beads and washed as described above, and the bound LpxC-ZZ was removed by incubation in 10 mM nitric acid overnight followed by ICP-MS analysis of metal ions in the eluate.

Native LpxC Deacetylase Activity—Chemically Defined Medium (CDM) (36) (supplemented with 0–20 μM $ZnSO_4$ and/or ferric ammonium citrate) was inoculated with BL21(DE3) cells and grown in a shaker (250 rpm) overnight at 37 °C. The cells were harvested by centrifugation, and the cell pellets resuspended in 20 mM Bistris propane, 10 mM TCEP, pH 7.5. The cells were washed, lysed, and clarified as described for the pulldown assays above. Metal ion concentrations in the cleared lysate were determined by ICP-MS analysis. The cleared lysate was diluted 10-fold into assay buffer prior to measurement of activity (see below) using 200 nM substrate. The LpxC activity in the cleared lysates was measured either immediately in the glove box or after 2.5 h of incubation in air. The ratio of iron and zinc bound to LpxC was estimated from the activity measured either anaerobically (A_0), reflecting the activity of both ZnLpxC and FeLpxC, or after 2.5 h of incubation in air ($A_{2.5}$) reflecting the activity due to ZnLpxC, assuming that all of the FeLpxC forms ZnLpxC under these conditions (18). Equation 1 was used to describe the activity at A_0, where S_{Zn} and S_{Fe} are the specific activity of Zn- and FeLpxC, respectively, whereas E_{Zn} and E_{Fe} are the concentration of Zn- and FeLpxC, respectively. Using the ~6-fold higher activity of FeLpxC relative to ZnLpxC ($E_{Fe}/E_{Zn} = 6$) (18), A_0 was solved in terms of the zinc enzyme and E_{tot} (Equation 2). Using the relationship $A_{2.5} = S_{Zn} \cdot E_{tot}$, the E_{Fe}/E_{tot} ratio in the anaerobic sample was calculated (Equation 3), and the E_{Fe}/E_{Zn} ratio was obtained by conservation of mass. To demonstrate that the native activity observed was specifically due to LpxC activity, control assays were performed with the LpxC-specific hydroxamate inhibitor L-161,240 (18).

$$A_0 = S_{Zn}E_{Zn} + S_{Fe}E_{Fe} \quad \text{(Eq. 1)}$$

$$\frac{A_0}{E_{Tot}} = 6S_{Zn} - 5S_{Zn}\frac{E_{Zn}}{E_{Tot}} \quad \text{(Eq. 2)}$$

$$\frac{E_{Zn}}{E_{Tot}} = \frac{6A_{2.5} - A_0}{5A_{2.5}} \quad \text{(Eq. 3)}$$

LpxC Assay—LpxC activity was measured as described previously (16, 37, 38). For native activity measurements, assays were performed in 20 mM Bistris propane, 10 mM TCEP, pH 7.5, bovine serum albumin (BSA, fatty acid-free, 1 mg/ml), and [^{14}C]UDP-3-*O*-(3-hydroxymyristoyl)-*N*-acetyl-glucosamine (200 nM). Mixtures were pre-equilibrated at 30 °C, and the reactions were initiated by the addition of cell lysate. LpxC assays were also carried out in Fe(II) buffers for affinity determinations, as described below. After incubation for various times, the reactions were quenched by the addition of sodium hydroxide, which also cleaves the myristate substituent for ease of separation. Substrate and product were separated on PEI-cellulose TLC plates (0.1 M guanidinium HCl) and quantified by scintillation counting. Initial rates of product formation (<20% reaction) were determined from these data.

In Vitro Metal Ion Affinity and Exchange—To remove contaminating metal ions, ultrafiltration devices (Microcon molecular weight cutoff of 30,000) were incubated with 10 mM Hepes, pH 7.5, 500 μM EDTA, 100 mM dipicolinic acid for 30 min (500 μl), followed by 3× 500-μl washes with ultrapure water. To examine metal exchange *in vitro*, 10 μM LpxC C63A with either bound Zn(II) or Fe(II) was incubated in an anaerobic chamber with various concentrations of $ZnSO_4$ or $FeCl_2$ (0–300 μM) for ≥15 min in 20 mM Bistris propane, pH 7.5, 10 mM TCEP. The free and bound metal ions were separated by centrifugation (3000 × *g*, 4 min) in an ultrafiltration device, and the metals in an equal volume of filtrate and retentate were then analyzed by ICP-MS.

For Zn(II) affinity measurements, apo-LpxC C63A (1–200 μM) was incubated in a metal ion and pH buffer containing 1 mM nitrilotriacetic acid (NTA), 5 mM Mops, pH 7, 2.5 μM dipic-

olinic acid, and 0–0.5 mM Zn_{tot} (0–3.3 nM Zn_{free}) at 30 °C for 30 min in an anaerobic chamber (39, 40). Free and bound metal were separated by ultrafiltration, described above, and metal ions were measured by ICP-MS. The concentration of Zn_{free} in the metal buffers was calculated using the program MINEQL+ (Environmental Research software). The value of K_D^{Zn} was obtained by fitting a binding isotherm to these data.

The affinity of LpxC for Fe(II) was measured by assaying catalytic activity in the presence of varying free Fe(II) concentrations in an anaerobic glove box in 1 mM NTA, 5 mM Mops, pH 7, serving as both a pH and metal buffer. The assays contained 0–950 μM total iron $(Fe(II)_{free}$ 0–2.6 μM, as calculated by MINEQL+ (Environmental Research Software)), and 10 nM LpxC, in the presence of 1 mg/ml BSA. The Fe(II) affinity of LpxC was unchanged by pre-equilibrating the BSA with a buffered Fe(II) solution. The assay mixtures, containing all components except substrate, were incubated for 4 h on ice followed by 30 min at 30 °C in the anaerobic glove box. Assays were initiated by the addition of substrate (200 nM final), and processed as described above. The affinity is not dependent on the concentration of metal buffer.

Metal Dissociation Rates—The first order rate constant for Me(II) dissociation from LpxC was measured by the time-dependent loss of activity upon incubation with EDTA. LpxC reconstituted with stoichiometric Zn(II) or Fe(II) was diluted into assay buffer containing 1 mM EDTA at 30 °C. At various times (0–30 min) an aliquot was diluted 100-fold into assay buffer (2 nM LpxC, 200 nM substrate). The reactions were quenched by the addition of sodium hydroxide and analyzed as described above. A single exponential was fit to the initial rates as a function of time. To measure the effect of fatty acids on metal dissociation kinetics, 100 μM palmitate was incubated with Me(II)-LpxC for 1 h on ice prior to dilution into EDTA at 30 °C.

RESULTS

LpxC Purified from E. coli Contains Mainly Bound Fe(II)—LpxC purified from *E. coli* was previously shown to contain bound Zn(II); however, this protein was purified under aerobic conditions with 2 mM dithiothreitol as the reducing agent (15), which is not sufficient to prevent oxidation of bound Fe(II) (18). Subsequent experiments demonstrated that under anaerobic conditions Fe(II)-bound LpxC is 6–8-fold more active than ZnLpxC (18). The absorbance spectrum of Fe(II)-bound LpxC has a broad peak with a maximum at 420 nM (ϵ_{420} = 1080 M^{-1} cm^{-1}) (supplemental Fig. S1), similar to the spectra of other low spin non-heme Fe(II) complexes (41, 42) and consistent with the extended x-ray absorption fine structure data suggesting pentacoordinate metal geometry (18).

To clarify the identity of the biologically relevant metal ion cofactor, we purified LpxC under anaerobic conditions to re-examine the identity of the native metal cofactor. For all of these experiments, we used a previously characterized LpxC variant, EcC63A (18), that has high catalytic activity but reduced affinity for metal ions at the inhibitory site. This protein was fused to a cleavable C-terminal ZZ tag (33–35) (EcLpxCC63A-Tev-ZZ or LpxC-ZZ) to facilitate rapid purification of LpxC from crude cell lysates with minimal metal contamination. LpxC-ZZ was induced in BL21(DE3) cells grown in minimal medium containing varied metal supplements and rapidly isolated by incubation with IgG beads followed by elution with either nitric acid or TEV protease. The concentration of metals and protein in the column eluate were determined by ICP-MS and Bradford assays, respectively. This method minimizes contamination of LpxC by adventitious metal ions. Control experiments using cells containing LpxC without the ZZ tag demonstrate that little or no (<0.1 μM) protein or metal ions are observed in the eluate. In general, LpxC-ZZ co-purifies with mainly Fe(II) and some Zn(II) (Table 1); no other divalent metal ions (*e.g.* cobalt, nickel, and copper) are observed at greater than trace levels (<3–5%). A substoichiometric metal ratio is also observed under all conditions, suggesting either that LpxC-ZZ is not fully saturated with metals under physiological conditions or metal ions dissociate during the purification steps. This latter possibility is further examined in control experiments described below. Calculations based on metal affinities (see under "Discussion") also rationalize the substoichiometric metal bound to LpxC under some conditions. LpxC-ZZ purified from cells grown in minimal (CDM) medium with or without iron supplementation contains mainly bound iron (Table 1); however, supplementation of the medium with zinc increases the iron/zinc ratio bound to LpxC-ZZ. In fact, the iron/zinc ratio bound to LpxC-ZZ varies with the $(iron/zinc)_{total}$ ratio in the cell lysate in a roughly linear fashion (Fig. 2*A*), suggesting that LpxC co-purifies with the most abundant metal ion in the cells. The same trend is observed when the cellular concentration of LpxC is decreased (Fig. 2*A*), indicating that the metal content is not an artifact of protein overexpression.

TABLE 1
Metal stoichiometry of EcC63A LpxC-ZZ purified from *E. coli*
EcC63A LpxC-ZZ was purified as described under "Materials and Methods." The bound metal concentrations were determined by ICP-MS analysis, and the protein concentration was measured using a Bradford assay.

Growth medium	Lysate Fe/Zn ratio	FeLpxC/E_{tot}[a]	ZnLpxC/E_{tot}[a]
CDM[b]	3.2	0.41 ± 0.11	0.08 ± 0.01
+Fe[b]	22	0.59 ± 0.14	0.04 ± 0.01
+Zn[b]	0.34	0.10 ± 0.07	0.25 ± 0.07
+Fe and Zn[b]	2.9	0.42 ± 0.10	0.10 ± 0.06

[a] Data represent the average and S.D. from two replicate experiments. Data for LpxC isolated from cells grown in varied metal concentrations are shown in Fig. 2*A*. ICP-MS data have S.E. of ±5%.
[b] Chemically defined medium was without metal supplements or supplemented with 20 μM $ZnSO_4$, 20 μM ferric ammonium citrate, or both.

One possible explanation of the correlation between the metals bound to LpxC-ZZ and the metal content of the cell lysate is that the metals bound to LpxC equilibrate with the cell lysate after cell lysis. To examine this possibility, LpxC-ZZ reconstituted with either stoichiometric Zn(II) or Fe(II) was incubated with cell lysates, purified using IgG beads, and the bound metal content determined by ICP-MS. These experiments demonstrate that the metal ion bound to LpxC-ZZ does not significantly dissociate (stoichiometry >0.7 Me(II)/LpxC) or equilibrate with metals in the cell lysate during the pulldown procedure because the iron/zinc ratio depends on the identity of the original metal ion bound to LpxC (Fig. 2*B*). Consequently, the pulldown experiments measure the bound metal content of LpxC-ZZ expressed in *E. coli* when cells are lysed

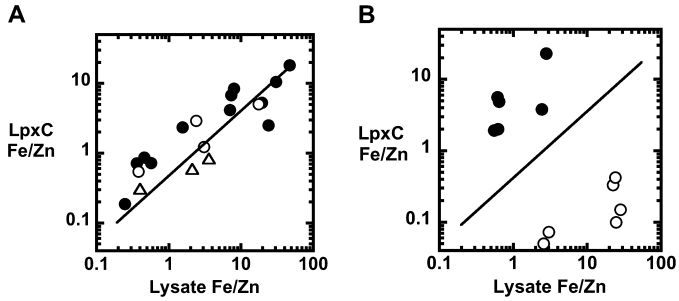

FIGURE 2. **Metal content of EcC63A LpxC-ZZ isolated from *E. coli*.** *A,* EcC63A LpxC-ZZ was expressed in BL21(DE3) pEcC63ALpxC-ZZ *E. coli* grown in minimal medium with and without iron or zinc supplementation (5–20 μM) and induced by addition of either 1 mM isopropyl β-D-thiogalactopyranoside (*closed circles*) or 0.1 mM isopropyl β-D-thiogalactopyranoside (*open circles*). The protein was purified using an IgG pulldown under anaerobic conditions (see "Materials and Methods"). The iron/zinc ratio of metals bound to LpxC-ZZ (*circles*) and in the cleared lysate was analyzed by ICP-MS. The iron/zinc ratio in natively expressed LpxC determined by activity (*triangles*), as described in the legend of Fig. 3, mirror the pulldown data. *B,* as controls, purified FeLpxC-ZZ (*closed circles*) or ZnLpxC-ZZ (*open circles*) was added to lysates of BL21(DE3) pEcC63ALpxC *E. coli* cells grown in minimal medium with and without iron or zinc supplementation (5–20 μM) and repurified by IgG-pulldown, as described under "Materials and Methods." LpxC-ZZ retains the majority of the original metal ion and does not readily equilibrate with metal ions in the lysate. Trendline reflects data in *A*.

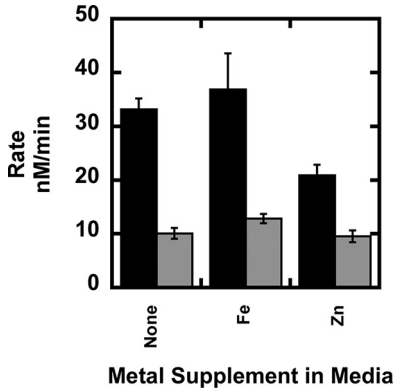

FIGURE 3. **Native LpxC activity varies with metal supplementation in the growth medium.** *E. coli* BL21(DE3) cells (without LpxC expression plasmid) were grown in minimal medium with and without 20 μM metal supplementation, lysed, and assayed for deacetylase activity as described under "Materials and Methods" either anaerobically (*black bars*) or after exposure to room oxygen for 2.5 h (*gray bars*).

and indicate that LpxC incorporates the most available metal ion in a manner reflective of the cellular iron/zinc ratio.

Native Activity Is Oxygen-sensitive and Dependent on Iron/Zinc$_{total}$—We have previously shown that LpxC activity in crude cell lysates from cells grown in LB medium is redox-sensitive, consistent with the presence of Fe(II)-LpxC (18). However, under anaerobic conditions, the activity of LpxC in cell lysates is stable for >30 min, demonstrating that the metal ions do not rapidly dissociate or exchange. To further examine the *in vivo* metal content of LpxC, we measured the redox sensitivity of the native LpxC activity of *E. coli* cell lysates (no overexpression of LpxC) prepared from BL21(DE3) cells grown in minimal medium supplemented with iron and/or zinc. The cells were lysed in an anaerobic chamber, and the LpxC activity was assayed immediately after lysis (reflecting the activity of both ZnLpxC and FeLpxC) as well as after sufficient incubation in air (2.5 h) to allow the Fe(II) cofactor bound to LpxC to oxidize and be replaced by Zn(II) (18). These data demonstrate that the ratio of Fe(II)-LpxC to Zn(II) (see "Materials and Methods") bound to natively expressed LpxC also depends on the (iron/zinc)$_{total}$ ratio in the cell lysate, comparable with the pulldown experiments reported above (Fig. 2*A*). Notably, the LpxC activity of cells grown in medium without metal supplementation is comparable with the activity measured in iron-supplemented cells (Fig. 3), confirming that native LpxC contains a bound Fe(II) cofactor in cells grown in minimal medium. Additionally, these data demonstrate that the correlation between the identity of the metal cofactor of native LpxC and the metal availability is not due to overexpression of LpxC-ZZ.

LpxC Binds Zinc More Tightly than Iron—To further clarify the metal ion selectivity of LpxC, we determined the affinities of the enzyme for Fe(II) and Zn(II) maintaining the metal concentration with metal ion buffers. Determination of the zinc affinity using ultrafiltration and ICP-MS analysis reveals a K_D of 60 ± 20 pM (Fig. 4*A* and Table 2). This value is comparable with the proposed cellular free Zn(II) concentrations (27, 28). The dissociation constant of LpxC for Fe(II), determined from enhancement of catalytic activity, is 110 ± 40 nM (Fig. 4*A* and Table 2). This value is lower than the estimated cellular free Fe(II) concentration (29, 43). These results predict that, despite the ~2000-fold higher affinity for Zn(II), Fe(II)-LpxC is the thermodynamically favored form of the enzyme under biological conditions due to the significantly higher concentration of cellular Fe(II)$_{free}$, which is consistent with the pulldown results (Table 1). Furthermore, binding of stoichiometric metal ion decreases the lability of C63A LpxC at elevated temperatures, as measured by a time-dependent decrease in the intrinsic protein fluorescence (supplemental Fig. S2). Addition of stoichiometric Zn(II) has a larger effect on the temperature-dependent lability of C63A apo-LpxC compared with Fe(II), consistent with the higher affinity of zinc.

To probe the exchange of bound metal cofactors, LpxC was reconstituted with either Fe(II) or Zn(II) and incubated with excess concentrations of the competing metal ion for 15 min, and then the identity of the bound metal ions was determined. These experiments demonstrate that the Fe(II) cofactor bound to LpxC readily exchanges with excess Zn(II) (Fig. 4*B*), although little exchange is observed when Zn(II)-LpxC is incubated with excess Fe(II). These data are consistent with the higher affinity of LpxC for zinc compared with iron, and the data can be modeled by competitive binding equations (Equations 4 and 5 and Fig. 4*B*) using the measured metal affinities. These calculations demonstrate that at the concentrations used for the *in vitro* exchange experiments, ZnLpxC is the predominant form at equilibrium.

$$\frac{E \cdot \mathrm{Fe}}{E_{\mathrm{Tot}}} = \frac{1}{1 + \frac{K_D^{\mathrm{Fe}}}{\mathrm{Fe}_{\mathrm{free}}}\left(1 + \frac{\mathrm{Zn}_{\mathrm{free}}}{K_D^{\mathrm{Zn}}}\right)} \qquad \text{(Eq. 4)}$$

$$\frac{E \cdot \mathrm{Zn}}{E_{\mathrm{Tot}}} = \frac{1}{1 + \frac{K_D^{\mathrm{Zn}}}{\mathrm{Zn}_{\mathrm{free}}}\left(1 + \frac{\mathrm{Fe}_{\mathrm{free}}}{K_D^{\mathrm{Fe}}}\right)} \qquad \text{(Eq. 5)}$$

The rate constants for dissociation of LpxC-bound metal ions were determined from the time-dependent decrease in

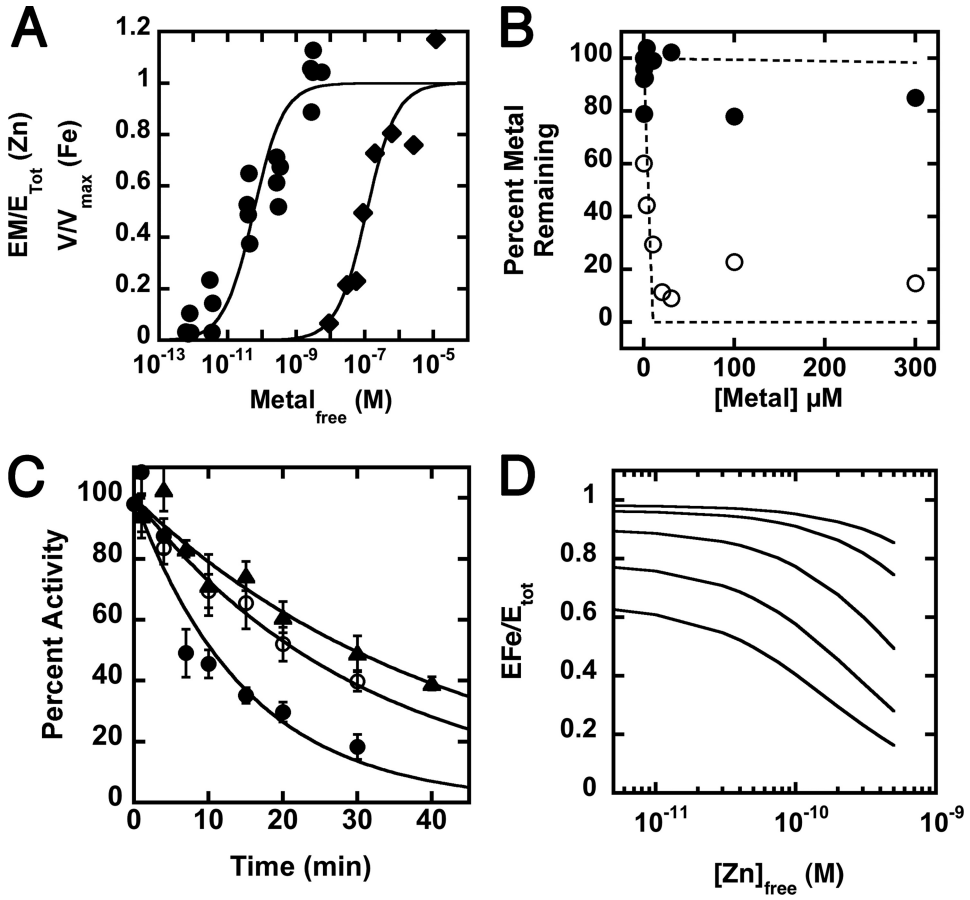

FIGURE 4. **C63A-LpxC readily equilibrates with metal ions *in vitro* and has a significantly higher affinity for Zn(II) than Fe(II).** *A,* affinity of C63A-LpxC for Zn(II) is 1800-fold higher than Fe(II). Apo-C63A-LpxC (untagged) was equilibrated with buffered metal solutions (5 mM Mops, 1 mM NTA, pH 7, as described under "Materials and Methods"). Bound zinc (*circles*) was analyzed by ultrafiltration and ICP-MS analysis, (K_D^{Zn}) and bound iron (*diamonds*) was analyzed by enhancement of LpxC activity (K_D^{Fe}) measured at 200 nM substrate, 30 °C, pH 7, as described under "Materials and Methods." A binding isotherm is fit to these data. *B,* LpxC metal ion dissociation occurs readily *in vitro*. 10 μM ZnLpxC (*closed circles*) or FeLpxC (*open circles*) in 20 mM BisTris, pH 7.5, was incubated with varying concentrations of competing metal ion, and then bound metal ions were determined by ultrafiltration followed by ICP-MS analysis, as described under "Materials and Methods." *Dashed lines* shown are simulations calculated from Equations 4 and 5 using the metal dissociation constants determined in *A*. *C,* 200 nM ZnLpxC (*open circles*), ZnLpxC + 100 μM palmitate (*triangles*), or FeLpxC (*closed circles*) was incubated in 1 mM EDTA, 20 mM BisTris, pH 7.5, 30 °C. At various times the deacetylase activity was measured by dilution (100-fold) into an assay containing 200 nM substrate, 1 mg/ml BSA, 20 mM BisTris, pH 7.5, 30 °C, as described under "Materials and Methods." A single exponential decay is fit to the data. *D,* metal bound to LpxC can switch between Fe(II) and Zn(II) depending on the free metal ion concentrations. The stoichiometry of Fe(II) bound to LpxC (E·Fe/E_{tot}) was calculated as a function of $[Zn]_{free}$ at 0.2, 0.4, 1, 3, or 6 μM $[Fe]_{free}$ ($[Fe]_{free}$ increases from the *bottom* to the *top curve*) using Equations 4 and 5 with the metal dissociation constants shown in Table 2.

TABLE 2
Kinetic and thermodynamic parameters of LpxC-C63A

Enzyme	$K_D^{metal\ ion}$	k_{cat}/K_m [a]
		$min^{-1}\ \mu M^{-1}$
Zn(II)-C63A LpxC	60 ± 20 pM[b]	170 ± 34
Fe(II)-C63A LpxC	112 ± 43 nM[b]	990 ± 130

[a] Data were adapted from Ref. 18.
[b] The affinity of LpxC-C63A for Zn(II) and Fe(II) was determined using ultrafiltration or activity measurements in buffered metal solutions at 30 °C pH 7, as described in the legend of Fig. 4.

activity upon dilution of the enzyme into EDTA and are not dependent on the concentration of chelator. These measurements reveal that the rate constant for dissociation (k_{off}) of Zn(II) and Fe(II) from LpxC are 0.032 ± 0.003 and 0.067 ± 0.004 min^{-1}, respectively (Fig. 4*C*). The similarity in the dissociation rate constants for Fe(II) and Zn(II) is unexpected given the significantly higher affinity of LpxC for Zn(II). Therefore, the discrimination between the two metal ions is observed mainly in the apparent association rate constants that are estimated from the values of K_D and k_{off} as ~9×10^6 (zinc) and 1×10^4 $M^{-1}\ s^{-1}$ (iron), assuming a one-step binding mechanism. Addition of palmitate to ZnLpxC slows the dissociation rate constant by ~1.3-fold to a half-time of 30 min at 25 °C suggesting that metal exchange in cell lysates could be inhibited by ligand binding. Although LpxC activity in cell lysates is stable under anaerobic conditions, addition of 1 mM EDTA to the lysate causes a 2-fold decrease in activity in 30 min, a time scale that is in the same range as the metal dissociation constants measured *in vitro*. These data suggest that EDTA decreases inhibition of metal exchange in lysates. Additionally, these data demonstrate that metals bound to LpxC can dissociate readily *in vitro*, disfavoring the possibility that *in vivo* metal selectivity is determined solely by a kinetic trap.

DISCUSSION

LpxC Is Activated by Either Fe(II) or Zn(II) in Cells—LpxC purified under aerobic conditions contains bound Zn(II) (15). However, LpxC is activated *in vitro* by a number of divalent metal ions, including zinc, iron, nickel, and cobalt (15, 18) and Fe(II)-LpxC is 6 – 8-fold more active than Zn(II)-LpxC (Table 2) (18). Substitution of Fe(II) for Zn(II) also enhances the affinity of LpxC for fatty acids by ~6-fold and the affinity for hydroxamate inhibitors by ~2-fold (18). X-ray absorption experiments demonstrate an increase in the ground state metal geometry from 4-coordinate in ZnLpxC to 5-coordinate in the Fe(II)-enzyme (18). These data suggest that enzyme function may correlate with coordination number; a 5-coordinate metal ion may enhance coordination of both water and substrate to lower the pK_a value of the metal-bound water and to polarize the carbonyl group of the substrate to enhance catalysis. Despite the higher activity of Fe(II)-LpxC under *in vitro* conditions, the metal cofactor that activates LpxC under cellular conditions was unclear.

In the presence of oxygen, the Fe(II) cofactor bound to LpxC is oxidized to Fe(III), which dissociates and is replaced by Zn(II)

(18). Therefore, to examine the *in vivo* metal content of LpxC, we developed a rapid pulldown experiment using an IgG-binding ZZ tag that could be carried out under anaerobic conditions. Subsequent determination of the bound metal by ICP-MS demonstrates that although the majority of metal bound to LpxC purified from cells grown in minimal medium is iron, the enzyme also contains bound zinc. In fact, the ratio of iron/zinc bound to LpxC-ZZ is linearly dependent on the iron/zinc ratio in the cell lysate (Fig. 2*A*). Control experiments (Fig. 2*B*) demonstrate that the measured LpxC metal content reflects the metals bound to LpxC *in vivo* when the cells are lysed. Furthermore, the iron/zinc ratio bound to natively expressed LpxC correlates with the iron/zinc ratio obtained from the pulldown assays (Fig. 2*A*), demonstrating that the observed metal variation in LpxC is not an artifact of protein overexpression. These data demonstrate that LpxC in *E. coli* binds and is activated by the "most available" metal ion. Therefore, although LpxC normally functions using Fe(II) as the co-factor, the metal cofactor switches to Zn(II) to adapt to environmental conditions and/or to regulate activity.

Metal Selectivity Is Determined by Association Kinetics and Thermodynamics—In contrast to the enhanced activity of Fe(II)-LpxC compared with Zn(II)-LpxC, the affinity of LpxC for Fe(II) is >1000-fold weaker than Zn(II) ($K_D \sim 100$ nM and 60 pM, respectively) (Fig. 4*A*). This differential affinity is consistent with the increased Lewis acidity and greater ligand stabilization energy predicted by the Irving-Williams series of metal stability constants (44, 45).

Unexpectedly, the rate constants for dissociation of Zn(II) and Fe(II) from the LpxC-metal complex are comparable (0.032 and 0.067 min^{-1}, respectively (Fig. 4*C*)) despite the large differential in binding affinity. This result indicates that metal selectivity occurs in the apparent association rate constant, estimated as 10^7 and 10^4 M^{-1} s^{-1} for Zn(II) and Fe(II), respectively, and implies that association of Fe(II) is not a diffusion-controlled step. Similar metal association kinetics have previously been observed for human carbonic anhydrase II where differential association rate constants for Zn(II) and Cu(II) (10^4–10^5 and 10^9 M^{-1} s^{-1}, respectively) have been observed (46, 47). Analysis of the zinc binding kinetics of human carbonic anhydrase II mutants suggests a two-step mechanism as follows: diffusion-controlled zinc association to form a complex with two protein ligands followed by a second slower step that includes coordination of the third protein ligand (48). A similar two-step mechanism could explain the kinetics for Fe(II) binding to LpxC.

Given the relatively facile dissociation of the active site metal under *in vitro* conditions ($t_{1/2}$ = 10–25 min), retention of the *in vivo* metal ion during purification of LpxC could have been difficult. However, little metal exchange or dissociation was observed in cell lysates (Fig. 2*B*) indicating that metal exchange/dissociation from LpxC is inhibited in lysates. One possible mechanism for this inhibition is the formation of a ternary LpxC-metal-ligand complex that decreases the metal dissociation rate constant. For example, a second metal ion or a fatty acid, such as palmitate (Fig. 4*C*), may bind to LpxC to inhibit metal exchange/dissociation (18, 37, 49).

Despite the higher affinity of LpxC for Zn(II), the *in vivo* data paradoxically indicate that Fe(II) is the predominant metal bound to LpxC in *E. coli* (Figs. 2 and 3 and Table 1). The mechanisms for determination of the iron/zinc metal selectivity of proteins in a cell are currently unclear. Metal selectivity has previously been proposed to depend on metal availability and/or be regulated by metallochaperones, although no zinc-specific metallochaperones have yet been identified (50, 51). As described in detail below, the observed *in vivo* metal content of LpxC can be rationalized solely from the metal affinity and concentration. Although the total cellular iron and zinc concentrations are comparable, at ~0.2 mM in most systems (26), the best estimates for the free or "readily exchangeable" cellular concentrations of Fe(II) and Zn(II) are vastly different. The best measurements, carried out mainly in mammalian cells, indicate that the concentration of $Zn(II)_{free}$ is 10–400 pM, although the concentration of $Fe(II)_{free}$ is 0.2–6 μM or higher (27–32). Therefore, the readily exchangeable Fe(II) concentration is predicted to be higher than the K_D^{Fe} for LpxC, although the readily exchangeable zinc concentration is near the K_D^{Zn}, rationalizing the predominance of Fe(II)-LpxC *in vivo*.

Using purely thermodynamic considerations, the percentage of iron- and zinc-bound LpxC can be calculated from the metal affinities and concentrations using a competitive model for LpxC metal binding (Equations 4 and 5). These calculations reveal that if metal binding to LpxC is under thermodynamic control, the balance of iron- to ZnLpxC is readily altered by changes in the free metal concentrations (Fig. 4*D*). For example, at the highest Fe_{free} and lowest Zn_{free} concentrations reported (6 μM and 10 pM, respectively), LpxC is calculated to contain 98% iron, 0.3% zinc, and 1.7% apoenzyme (iron/zinc ratio = 330). At the opposite extreme, 0.2 μM Fe_{free} and 400 pM Zn_{free}, LpxC is calculated to bind 19% iron and 70% zinc with 11% apoenzyme (iron/zinc ratio = 0.27). The measured values for Fe-, Zn-, and apo-LpxC in cells grown in CDM (Table 1) can be recapitulated using readily exchangeable cellular concentrations of Zn(II) and Fe(II) of 10 pM and 0.1 μM, respectively. These calculations indicate that the observed metal content of LpxC, including the substoichiometric metal content, can be explained solely using a thermodynamic model. Furthermore, these calculations demonstrate that modest perturbations in the cellular metal ion pool could influence the metal content of LpxC, as observed in response to alterations in the metal content of the media. Therefore, LpxC is well suited for metal switching *in vivo*. Importantly, this model for LpxC metal ion specificity demonstrates that thermodynamic considerations are sufficient to explain the observed behavior of LpxC *in vivo*. However, this correlation does not rule out the involvement of chaperones or other regulatory elements in determining the *in vivo* metal selectivity of LpxC.

Function of Metal Switching in LpxC—These data demonstrate that LpxC is the newest member of a growing class of non-heme Fe(II) hydrolases that were previously thought to be zinc enzymes, such as peptide deformylase, *S*-ribosylhomocysteinase, and possibly HDAC8 (19–24, 52, 53). However, LpxC should not be considered an Fe(II)-specific metalloenzyme but rather a Me(II)-dependent enzyme that is generally activated by Fe(II) but is subject to switching to

Zn(II)-LpxC in response to altered cellular conditions, such as variations in metal availability in the medium (Fig. 2*A*). Other environmental triggers, such as infection in a host or conditions of oxidative stress, may also perturb cellular metal ion homeostasis, and this alteration could be reflected in the active site metal ion bound to LpxC. Iron/zinc metal switching is likely to provide growth advantages under conditions where iron availability is limited, such as those encountered in infection (54–56). Metal switching may also be a novel regulatory mechanism, whereby the activity and possibly stability of LpxC can be finely tuned by changes in intracellular metal ion concentrations. Furthermore, it is possible that many prokaryotic metal-dependent hydrolases similarly switch the active site metal between Fe(II) and Zn(II) in response to changes in cellular metal homeostasis, as suggested by the enzymes previously identified as zinc- or iron-dependent hydrolases (21, 24, 57–60). This newly proposed mechanism to regulate the activity of LpxC and possibly other metalloenzymes has important implications for understanding metalloenzyme homeostasis as well as future drug design for LpxC and other antibiotic targets.

Acknowledgments—We gratefully acknowledge Dr. Ted Huston (University of Michigan Geological Sciences) for assistance with ICP-MS analysis and Prof. Christopher Walsh (Harvard Medical School) and Prof. Christian Raetz (Duke University) for the gift of ACP and LpxA plasmids, respectively. We also thank members of the Fierke laboratory for many thoughtful discussions and suggestions.

REFERENCES

1. Jackman, J. E., Fierke, C. A., Tumey, L. N., Pirrung, M., Uchiyama, T., Tahir, S. H., Hindsgaul, O., and Raetz, C. R. (2000) *J. Biol. Chem.* **275,** 11002–11009
2. Wyckoff, T. J., Raetz, C. R., and Jackman, J. E. (1998) *Trends Microbiol.* **6,** 154–159
3. Reeves, P. R., Hobbs, M., Valvano, M. A., Skurnik, M., Whitfield, C., Coplin, D., Kido, N., Klena, J., Maskell, D., Raetz, C. R., and Rick, P. D. (1996) *Trends Microbiol.* **4,** 495–503
4. Raetz, C. R., and Whitfield, C. (2002) *Annu. Rev. Biochem.* **71,** 635–700
5. Opal, S. M. (2007) *Int. J. Med. Microbiol.* **297,** 365–377
6. Manocha, S., Feinstein, D., Kumar, A., and Kumar, A. (2002) *Exp. Opin. Investig. Drugs* **11,** 1795–1812
7. Beall, B., and Lutkenhaus, J. (1987) *J. Bacteriol.* **169,** 5408–5415
8. Young, K., Silver, L. L., Bramhill, D., Cameron, P., Eveland, S. S., Raetz, C. R., Hyland, S. A., and Anderson, M. S. (1995) *J. Biol. Chem.* **270,** 30384–30391
9. Hernick, M., and Fierke, C. A. (2005) *Arch. Biochem. Biophys.* **433,** 71–84
10. Hernick, M., and Fierke, C. A. (2010) in *Comprehensive Natural Products II, Chemistry and Biology* (Mander, L., and Liu, H. W., eds) Vol. 8, pp. 547–581, Elsevier, Oxford
11. McClerren, A. L., Endsley, S., Bowman, J. L., Andersen, N. H., Guan, Z., Rudolph, J., and Raetz, C. R. (2005) *Biochemistry* **44,** 16574–16583
12. Mdluli, K. E., Witte, P. R., Kline, T., Barb, A. W., Erwin, A. L., Mansfield, B. E., McClerren, A. L., Pirrung, M. C., Tumey, L. N., Warrener, P., Raetz, C. R., and Stover, C. K. (2006) *Antimicrob. Agents Chemother.* **50,** 2178–2184
13. Barb, A. W., McClerren, A. L., Snehelatha, K., Reynolds, C. M., Zhou, P., and Raetz, C. R. (2007) *Biochemistry* **46,** 3793–3802
14. White, R. J., Margolis, P. S., Trias, J., and Yuan, Z. Y. (2003) *Curr. Opin. Pharmacol.* **3,** 502–507
15. Jackman, J. E., Raetz, C. R., and Fierke, C. A. (1999) *Biochemistry* **38,** 1902–1911
16. Hernick, M., Gennadios, H. A., Whittington, D. A., Rusche, K. M., Christianson, D. W., and Fierke, C. A. (2005) *J. Biol. Chem.* **280,** 16969–16978
17. McClerren, A. L., Zhou, P., Guan, Z., Raetz, C. R., and Rudolph, J. (2005) *Biochemistry* **44,** 1106–1113
18. Hernick, M., Gattis, S. G., Penner-Hahn, J. E., and Fierke, C. A. (2010) *Biochemistry* **49,** 2246–2255
19. Becker, A., Schlichting, I., Kabsch, W., Groche, D., Schultz, S., and Wagner, A. F. (1998) *Nat. Struct. Biol.* **5,** 1053–1058
20. Rajagopalan, P. T., and Pei, D. (1998) *J. Biol. Chem.* **273,** 22305–22310
21. Rajagopalan, P. T., Yu, X. C., and Pei, D. H. (1997) *J. Am. Chem. Soc.* **119,** 12418–12419
22. Groche, D., Becker, A., Schlichting, I., Kabsch, W., Schultz, S., and Wagner, A. F. (1998) *Biochem. Biophys. Res. Commun.* **246,** 342–346
23. Gantt, S. L., Gattis, S. G., and Fierke, C. A. (2006) *Biochemistry* **45,** 6170–6178
24. Zhu, J., Dizin, E., Hu, X., Wavreille, A. S., Park, J., and Pei, D. (2003) *Biochemistry* **42,** 4717–4726
25. Finney, L. A., and O'Halloran, T. V. (2003) *Science* **300,** 931–936
26. Outten, C. E., and O'Halloran, T. V. (2001) *Science* **292,** 2488–2492
27. Bozym, R. A., Thompson, R. B., Stoddard, A. K., and Fierke, C. A. (2006) *ACS Chem. Biol.* **1,** 103–111
28. Vinkenborg, J. L., Nicolson, T. J., Bellomo, E. A., Koay, M. S., Rutter, G. A., and Merkx, M. (2009) *Nat. Methods* **6,** 737–740
29. Petrat, F., de Groot, H., and Rauen, U. (2001) *Biochem. J.* **356,** 61–69
30. Espósito, B. P., Epsztejn, S., Breuer, W., and Cabantchik, Z. I. (2002) *Anal. Biochem.* **304,** 1–18
31. Meguro, R., Asano, Y., Odagiri, S., Li, C., Iwatsuki, H., and Shoumura, K. (2007) *Arch. Histol. Cytol.* **70,** 1–19
32. MacKenzie, E. L., Iwasaki, K., and Tsuji, Y. (2008) *Antioxid. Redox. Signal.* **10,** 997–1030
33. Nilsson, B., Forsberg, G., and Hartmanis, M. (1991) *Methods Enzymol.* **198,** 3–16
34. Nilsson, B., Moks, T., Jansson, B., Abrahmsén, L., Elmblad, A., Holmgren, E., Henrichson, C., Jones, T. A., and Uhlén, M. (1987) *Protein Eng.* **1,** 107–113
35. Löwenadler, B., Jansson, B., Paleus, S., Holmgren, E., Nilsson, B., Moks, T., Palm, G., Josephson, S., Philipson, L., and Uhlén, M. (1987) *Gene* **58,** 87–97
36. Outten, F. W., Outten, C. E., Hale, J., and O'Halloran, T. V. (2000) *J. Biol. Chem.* **275,** 31024–31029
37. Hernick, M., and Fierke, C. A. (2006) *Biochemistry* **45,** 14573–14581
38. Hernick, M., and Fierke, C. A. (2006) *Biochemistry* **45,** 15240–15248
39. McCall, K. A., and Fierke, C. A. (2000) *Anal. Biochem.* **284,** 307–315
40. McCall, K. A., and Fierke, C. A. (2004) *Biochemistry* **43,** 3979–3986
41. Grzyska, P. K., Müller, T. A., Campbell, M. G., and Hausinger, R. P. (2007) *J. Inorg. Biochem.* **101,** 797–808
42. Campos-Bermudez, V. A., Morán-Barrio, J., Costa-Filho, A. J., and Vila, A. J. (2010) *J. Inorg. Biochem.* **104,** 726–731
43. Epsztejn, S., Kakhlon, O., Glickstein, H., Breuer, W., and Cabantchik, I. (1997) *Anal. Biochem.* **248,** 31–40
44. Lippard, S. J., and Berg, J. M. (1994) *Principles of Bioinorganic Chemistry*, pp. 21–24, University Science Books, Mill Valley, CA
45. Irving, H., and Williams, R. J. (1948) *Nature* **162,** 746–747
46. Hunt, J. A., Ahmed, M., and Fierke, C. A. (1999) *Biochemistry* **38,** 9054–9062
47. Romans, A. Y., Graichen, M. E., Lochmüller, C. H., and Henkens, R. W. (1978) *Bioinorg. Chem.* **9,** 217–229
48. Kiefer, L. L., and Fierke, C. A. (1994) *Biochemistry* **33,** 15233–15240
49. Whittington, D. A., Rusche, K. M., Shin, H., Fierke, C. A., and Christianson, D. W. (2003) *Proc. Natl. Acad. Sci. U.S.A.* **100,** 8146–8150
50. Tottey, S., Harvie, D. R., and Robinson, N. J. (2005) *Acc. Chem. Res.* **38,** 775–783
51. Waldron, K. J., Rutherford, J. C., Ford, D., and Robinson, N. J. (2009) *Nature* **460,** 823–830
52. Chan, M. K., Gong, W., Rajagopalan, P. T., Hao, B., Tsai, C. M., and Pei, D. (1997) *Biochemistry* **36,** 13904–13909
53. Jain, R., Hao, B., Liu, R. P., and Chan, M. K. (2005) *J. Am. Chem. Soc.* **127,**

4558–4559
54. MacMicking, J., Xie, Q. W., and Nathan, C. (1997) *Annu. Rev. Immunol.* **15,** 323–350
55. Neilands, J. B. (1995) *J. Biol. Chem.* **270,** 26723–26726
56. Goetz, D. H., Holmes, M. A., Borregaard, N., Bluhm, M. E., Raymond, K. N., and Strong, R. K. (2002) *Mol. Cell* **10,** 1033–1043
57. Tripp, B. C., Bell, C. B., 3rd., Cruz, F., Krebs, C., and Ferry, J. G. (2004) *J. Biol. Chem.* **279,** 6683–6687
58. Seffernick, J. L., McTavish, H., Osborne, J. P., de Souza, M. L., Sadowsky, M. J., and Wackett, L. P. (2002) *Biochemistry* **41,** 14430–14437
59. D'souza, V. M., and Holz, R. C. (1999) *Biochemistry* **38,** 11079–11085
60. Porter, D. J., and Austin, E. A. (1993) *J. Biol. Chem.* **268,** 24005–24011